THE JOURNAL OF
PHYSICAL CHEMISTRY A

Article

pubs.acs.org/JPCA

A Closure Study of the Reaction between Sulfur Dioxide and the Sulfate Radical Ion from First-Principles Molecular Dynamics Simulations

Narcisse T. Tsona,[†] Nicolai Bork,[†,‡] Ville Loukonen,[*,†,§] and Hanna Vehkamäki[†]

[†]Division of Atmospheric Sciences, Department of Physics, University of Helsinki, P.O. Box 64, FI-00014 University of Helsinki, Finland

Supporting Information

ABSTRACT: In a previous study, we applied quantum chemical methods to study the reaction between sulfur dioxide (SO_2) and the sulfate radical ion (SO_4^-) at atmospheric relevant conditions and found that the most likely reaction product is $SO_3SO_3^-$. In the current study, we investigate the chemical fate of $SO_3SO_3^-$ by reaction with ozone (O_3) using first-principles molecular dynamics collision simulations. This method assesses both dynamic and steric effects in the reactions and therefore provides the most likely reaction pathways. We find that the majority of the collisions between $SO_3SO_3^-$ and O_3 are nonsticking and that the most frequent reactive collisions regenerate sulfate radical ions and produce sulfur trioxide (SO_3) while ejecting an oxygen molecule (O_2). The rate of this reaction is determined to be 2.5×10^{-10} cm^3 s^{-1}. We then conclude that SO_4^- is a highly efficient catalyst in the oxidation of SO_2 by O_3 to SO_3.

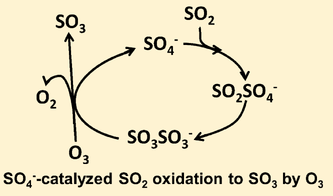

INTRODUCTION

Sulfur plays an important role in the chemistry of the atmosphere by influencing acid precipitation, aerosol particles, and clouds formation through sulfuric acid, the most oxidized sulfurous compound in the atmosphere. Sulfuric acid is mainly formed by electrically neutral oxidation of SO_2, the most abundant atmospheric sulfurous molecule.[1] Ionic oxidation of SO_2 generally leads to various different oxysulfur intermediate ions.[2−8] These ions are susceptible for triggering new reactions as the ionic oxidation of SO_2 is more complex than its neutral counterpart. To completely understand the atmospheric sulfur cycle, it is necessary to identify the different pathways of the reactions possibly initiated by the oxysulfur anions.

Recent studies have shown how some oxysulfur anions are converted during the process of sulfur oxidation in the atmosphere. For example, using ab initio calculations, Bork et al.[5] demonstrated that by colliding with O_3, SO_5^- is either decomposed into O_3^-, SO_3, and O_2 or converted into SO_4^-. In our previous quantum chemical studies, we found that SO_4^- reacts fast with SO_2 at standard conditions, especially at low relative humidity, forming the $SO_3SO_3^-$ product, which was shown to be stable toward decomposition into the initial reactants or SO_3 and SO_3^-.[8] Although further chemistry of the $SO_3SO_3^-$ ion was not clearly established from earlier studies, it likely depends on the collisions with the most abundant trace atmospheric oxidants such as O_3.

Currently the most commonly used theoretical approach to study chemical reactions is the use of quantum chemical methods. These methods consist of optimizing molecular structures to find the best possible arrangement of atomic nuclei and electrons and the corresponding ground state energy. The optimizations are done at $T = 0$ K, and the thermodynamical parameters are generally extrapolated to atmospheric temperature, e.g., 300 K under the harmonic oscillator-rigid rotor approximation. When the reaction proceeds through transition state configurations, different methods are usually used to determine the structure of the transition state, one of which consists of constraining some reaction coordinates while optimizing the remainder of the structure. This approach becomes extremely difficult when the transition state involves more than two species.

As an alternative approach, first-principles molecular dynamics collision simulations are a powerful tool to study chemical reactions. This method allows the system to evolve in time using forces calculated from the electronic structure, and the positions of the atomic nuclei are determined by solving Newton's equations of motion. We applied this method, which assesses both steric and dynamic effects in reactions as demonstrated by Bork et al.,[6] to investigate the pathways arising from $SO_3SO_3^-$ and O_3 collisons at atmospheric conditions. Different geometric orientations as well as the effect of water were considered in these collisions.

METHODS

All calculations were performed using the Quickstep module[9] of the CP2K package (www.cp2k.org). We utilized both atom-centered Gaussian and plane-wave basis sets to describe the electronic structure of the system.[10] Augmented, doubly polarized, triple-ζ basis sets (aug-TZV2P)[11] were used to represent the wave functions, and plane wave basis sets truncated at 400 Ry were used to describe the electronic

Received: December 18, 2015
Revised: January 29, 2016
Published: January 29, 2016

DOI: 10.1021/acs.jpca.5b12395

density. A cell size of 30 × 30 × 30 Å ^{3} was used in all simulations. Pseudopotentials[12] were used for core electrons, and 10^{-6} Hartrees was used as the convergence criterion for the wave function.

Although density functional theory (DFT) is not the most accurate method to describe intermolecular interactions such as dispersion, this method has been proven suitable for studying chemical reactions and to be a good compromise between accuracy and computation time. The density functional by Perdew, Burke, and Ernzerhof (PBE)[13] was used in this study with the D3 correctional scheme by Grimme et al.[14] to account for the incomplete treatment of dispersion forces by DFT. Recent studies showed that the PBE functional describes well the structures and energetics of various systems, especially when used with the dispersion correction.[15−17]

Initial structures for the systems were taken from our previous work[8] and reoptimized in CP2K with the above-mentioned density functional and basis set. We found earlier that the $SO_3SO_3^-$ ion is able to bind two water molecules under atmospherically relevant temperatures and humidities and, hence, 0−2 water molecules were included in the system investigated in this work. Initial velocities of all atoms of the molecular ion were obtained by performing short *NVT*-ensemble simulations at a constant temperature of 300 K, whereas impact velocities of the O_3 molecule were determined from the Maxwell−Boltzmann distribution of speeds, given in the Supporting Information. The O_3 molecule was initially placed about 5 Å from the cluster ion, in the six Cartesian directions. We obtained altogether 12 starting configurations in the absence of water. Due to multiple configurations for the hydrated $SO_3SO_3^-$ ion, there were 24 and 36 starting configurations for systems with one and two water molecules, respectively. Figure 1 shows one example of initial geometry for a simulation including two water molecules. The electron density of this configuration confirms that the extra electron is initially distributed on the $SO_3SO_3^-$ ion.

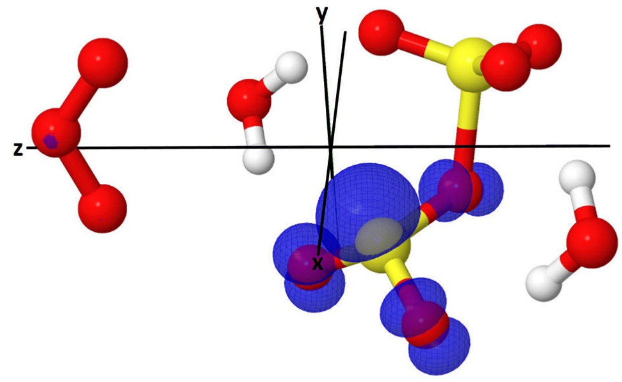

Figure 1. Example of initial configuration of the reactant system. The directions of ozone impact are along the Cartesian directions (±*X*, ±*Y*, ±*Z*). The spin density (in blue) is initially located at one end of the $SO_3SO_3^-$ ion. Yellow is sulfur, red is oxygen, and white is hydrogen.

All simulations were parallelized on 96 processors and performed in the *NVE* ensemble. A time step of 0.5 fs was used. The simulations were initially run between 2000 and 2500 MD steps. In the cases where no decisive outcome occurred within that time, the simulations were continued for another 2000−2500 MD steps run.

RESULTS AND DISCUSSION

A summary of all outcomes is shown in Table 1, and four of the most common end results are given by reactions R1a−d. Most of the collisions were nonsticking (reaction R1a), occurring in 41 out of 72 simulations. A collision is defined to be nonsticking when the colliding species approach each other and do not bind in any way leading to a reaction or cluster formation. In the nonsticking collisions, we found that either O_3 leaves the system as soon as it gets at a distance of 3 Å from the $SO_3SO_3^-$ ion or all molecules of the system fall apart as they approach each other. This mainly occurred when the impacting O_3 was moving in the direction of the oxygen molecules of the $SO_3SO_3^-$ ion. In these cases, the collisions were characterized by strong oxygen−oxygen repulsion. Nevertheless, some of such collisions led to significant geometric reorientations after a long run and eventually ended up as reaction R1b or reaction R1c. Reaction R1b, which led to the formation of $SO_4^-(H_2O)_{0-2}$, SO_3, and O_2, was the second most frequent outcome of all the collisions, occurring 20 times. Reaction R1c, which led to the formation of $[(SO_3SO_3)(O_3)(H_2O)_{0-2}]^-$, occurred in 9 simulations, and reaction R1d, leading to the formation of $[(HSO_4)(SO_3)(HO_3)(H_2O)]^-$, occurred in 2 simulations, and in the two water systems exclusively. The optimized Cartesian coordinates of all the reaction products are shown in the Supporting Information.

Table 1. Summary of the Outcome of All O_3 and $SO_3SO_3^-(H_2O)_n$ Collisions

	n			
outcome	0	1	2	total
no sticking	8	17	16	41
$SO_3 + SO_4^-(H_2O)_n{}^+ + O_2$	4	5	11	20
$[(SO_3SO_3)(O_3)(H_2O)_n]^-$		2	7	9
$[(HSO_4)(SO_3)(HO_3)(H_2O)]^-$			2	2
total	12	24	36	72

$$SO_3SO_3^-(H_2O)_{0-2} + O_3 \rightarrow \begin{cases} \text{no sticking} & \text{(a)} \\ SO_4^-(H_2O)_{0-2} + SO_3 + O_2 & \text{(b)} \\ [(SO_3SO_3)(O_3)(H_2O)_{0-2}]^- & \text{(c)} \\ [(HSO_4)(SO_3)(HO_3)(H_2O)]^- & \text{(d)} \end{cases} \qquad \text{(R1)}$$

Effects of Hydration and Direction of Impact. The effect of hydration was investigated for reaction R1b, the most frequent outcome leading to a chemical reaction. Considering a total of 12 simulations without water, 8 were nonsticking and 4 led to reaction R1b, resulting in a reaction percentage of 33%. The percentage of collisions leading to reaction R1b was 21% and 31% for systems containing one and two water molecules, respectively. This indicates that water has a slight hindering, though loose, effect toward reaction R1b. It is likely that water either shields $SO_3SO_3^-$ from the approach of O_3 or reduces the net ion−dipole interaction between $SO_3SO_3^-$ and O_3.

To have an estimate of the effect of impact direction on the outcome of the collisions, we chose the dihydrate as our model system. Two main directions for O_3 impact were considered: one toward the water molecules in the system and the other toward the $SO_3SO_3^-$ ion. When O_3 approached the system in the direction of $SO_3SO_3^-$, a significant fraction (37% of the total collisions in that direction) of collisions led to reaction R1b. However, the majority of collisions in the direction of water molecules did not lead to the formation of new products. In this direction, either the species formed a cluster (reaction R1c) or they did not stick, in accordance with Falsig et al.[18] and Ma et al.[19] We found that, of the total collisions in the direction of water, 36% were nonsticking (reaction R1a), 29% led to cluster formation (reaction R1c), 21% led to reaction R1b, and 14% led to reaction R1d.

In most of the collisions leading to reaction R1c, the systems were equilibrated after about 1000 fs. Running for additional time led to little configuration changes. Nevertheless, four of these systems that contained two water molecules were followed for longer simulation runs, ca. 2000−2500 steps. They led to O_3 evaporation from the cluster, whereas SO_3^- and SO_3 remained in strong interaction with each other. Hence we concluded that most, if not all, of the products of reaction R1c could end up decomposing into above-mentioned species. The further chemistries of SO_3^- and SO_3 are known. SO_3^- reacts fast with O_2 to form SO_5^- whereas SO_3 hydrolyses in a cluster with water to form sulfuric acid in the atmosphere.[2,20]

Reaction R1d occurred only when there were two water molecules in the system. Indeed, one of the water molecules acts as a bridge between O_3 and one end of the $SO_3SO_3^-$ ion, wherefrom a proton is transferred from water to O_3 (forming HO_3) and the remainder OH was transferred to SO_3 (forming the HSO_4 fragment). The chemical fates of the products of Reaction R1d are relatively well known although the HO_3 species has not been investigated extensively due to its elusive character.[21−23]

Energetics and Reaction Rate. The thermodynamics of reactions R1a−d are shown in Table 2. It can be seen that

Table 2. Thermodynamic Data of the O_3 + $SO_3SO_3^-(H_2O)_n$ Reaction, Calculated at the PBE-D3/aug-TZV2P Level of Theory[a]

n	ΔG	ΔH
	$SO_4^-(H_2O)_n$ + SO_3 + O_2	
0	−46.9	−33.2
1	−48.1	−35.2
2	−51.2	−38.5
	$[(SO_3SO_3)(O_3)(H_2O)_n]^-$	
0	11.4	−1.2
1	10.6	−2.7
2	8.9	−3.5
	$[(HSO_4)(SO_3)(HO_3)(H_2O)]^-$	
	−39.8	−53.7

[a] The main products are indicated. Gibbs free energies are calculated at 300 K, and units are kcal/mol.

reactions R1b and R1d are energetically favorable with Gibbs free energy changes as low as −40 kcal/mol. The structures corresponding to initial reactants, transition state, and products for a representative example of collisions leading to reaction R1b are shown in Figure 2. The electron density is also shown and it is seen that the extra electron, initially located at the $SO_3SO_3^-$, partially migrates to O_3 in the transition state and is finally on SO_4^- in the newly formed products. The antibonding π^* orbital of the oxygen molecule is also visible in the products. The energetics of few cases of reaction R1b are shown on Figure 3 wherefrom it can be seen that the reactions occur in about 280−400 fs and are accompanied by a significant release in potential energy. During the reaction, the potential energy drops by ca. 25−40 kcal/mol. Though the selected cases presented in Figure 3 show that the energy release increases with increasing hydration, this is not the general trend observed when all the cases investigated are explored. We found that the number of water molecules in the system seems to have no significant effect on the reaction time. The released potential energy is converted into kinetic energy, which is mainly manifested in vibration. As a direct consequence, the newly formed products remain vibrationally excited until they eventually collide with other species, whereas the O_2 molecule is rapidly ejected from the system. Because reaction R1d occurs only in 2 out of 72 simulations, the reaction rate of the collision between O_3 and $SO_3SO_3^-(H_2O)_{0-2}$ can be regarded as the rate of reaction R1b.

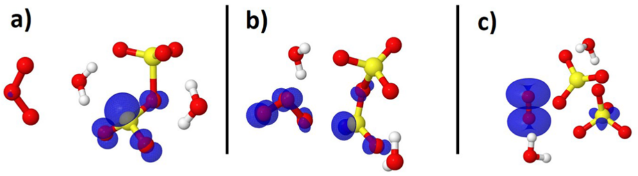

Figure 2. Structures corresponding to the (a) reactants, (b) transition state, and (c) newly formed products in one simulation leading to reaction R1b. The spin density is depicted in blue. Sulfur is yellow, oxygen is red, and hydrogen is white.

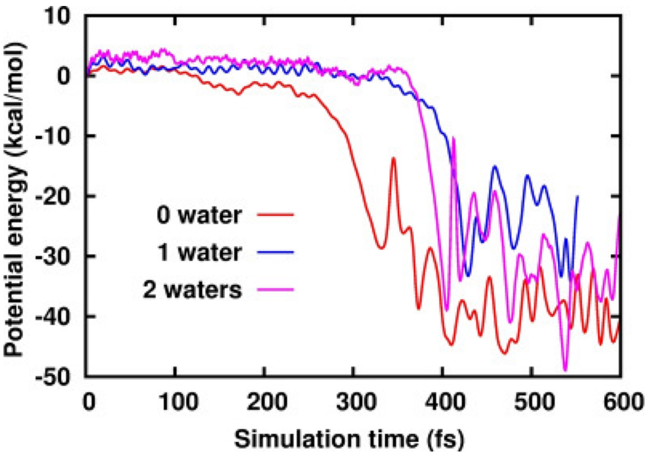

Figure 3. Potential energy of three reactive simulations (reaction R1b) as representative examples of simulations with zero, one, and two water molecules.

Overall, reaction R1b occurred in 4 out of 12 simulations in the absence of water, 5 out of 24 simulations, and 11 out of 36 simulations in the presence of one and two water molecules, respectively. The reaction rate constants are thus estimated to be 33%, 21%, and 31% of the collision rate constant of O_3 and $SO_3SO_3^-(H_2O)_n$ in the presence of 0, 1, and 2 water molecules, respectively. The collision rate constants are calculated from the parametrization by Su and Chesnavich,[24] given by

$$k_{R1} = \beta^{L} \times \left(\frac{(x + 0.5090)^2}{10.526} + 0.9754 \right) \quad (1)$$

where $\beta^L = q\mu^{-1/2}(\pi\alpha/\epsilon_0)^{1/2}$, $x = \mu_D/(8\pi\epsilon_0\alpha k_B T)^{1/2}$, q is the charge of the ion, μ is the reduced mass of the colliding species, and α and μ_D are the polarizability and dipole moment of the polar molecule. All numerical values of the parameters used in eq 1 are given in the Supporting Information. The overall rate constant of reaction R1b, $k_{R1b,av}$, calculated while taking into account the relative concentration of the $SO_3SO_3^-$ hydrates, is given by

$$k_{R1b,av} = k_{R1b,0w} \times C_{0w} + k_{R1b,1w} \times C_{1w} + k_{R1b,2w} \times C_{2w} \tag{2}$$

where $k_{R1b,iw}$ is the reaction rate constant of reaction R1b in the presence of i water molecules and C_{iw} is the relative concentration of the $SO_3SO_3^-(H_2O)_i$ ion at given temperature and relative humidity. The relative concentrations are calculated from the law of mass action using the hydration Gibbs free energies of $SO_3SO_3^-$ (calculations are shown in the Supporting Information). At 300 K and 50% relative humidity, with 95% confidence interval, we found an overall rate constant of 2.5×10^{-10} cm^3 s^{-1} for reaction R1b. The magnitude of the obtained rate constant implies that the decomposition of $SO_3SO_3^-$ by O_3 into SO_4^-, SO_3, and O_2 (reaction R1b) is fast under the investigated temperature and relative humidity. Furthermore, this rate can be considered as the lower limit because part of the collisions leading to cluster formation may end up as reaction R1b.

The formation of $SO_3SO_3^-$ from the SO_4^- + SO_2 reaction was determined to be fast and energetically favorable at 300 K and low relative humidity (below 20%).[8] Combining this reaction to reaction R1b leads to the overall reaction

$$SO_2 + O_3 \rightarrow SO_3 + O_2 \tag{R2}$$

where SO_4^- acts as a catalyst in the oxidation of SO_2 by O_3 to SO_3.

CONCLUSION

The chemical fate of $SO_3SO_3^-$, the most likely product of SO_2 + SO_4^- reaction at 300 K and low relative humidity, was investigated by reaction with ozone using first-principles molecular dynamics collision simulations. This method, through the inclusion of the dynamic and steric effects, scans most of the collision possibilities. The simulations were performed in the *NVE* ensemble.

We found that 22 out of 72 simulations lead to reactions whereas the remainder of the collisions either are not sticking (41 simulations) or lead to a cluster formation (9 simulations). The most frequent reactive collision was the one leading to SO_4^- + SO_3 + O_2 products (reaction R1b). The products were formed with a significant release in potential energy. This reaction happened 19 times. We found that when the impacting ozone molecule is moving in the direction of a water molecules in the system, nonsticking collision events prevail, whereas when the ozone molecule is moving in the direction of the $SO_3SO_3^-$ atoms, reaction R1b is favored. Because $SO_3SO_3^-$ is formed from SO_2 and SO_4^- collisions, we conclude that SO_4^- is a catalyst for the oxidation of SO_2 by O_3 to SO_3.

The current results allow us to provide an estimate of the rate constant of reaction R1b. We find that at 300 K and 50% relative humidity and with 95% confidence interval, the lower limit of the reaction rate constant is 2.5×10^{-10} cm^3 s^{-1}. The overall effect of water is seen to slightly lower the reaction rate by shielding the O_3–$SO_3SO_3^-$ ion–dipole interaction.

ASSOCIATED CONTENT

Supporting Information

The Supporting Information is available free of charge on the ACS Publications website at DOI: 10.1021/acs.jpca.5b12395.

Cartesian coordinates of the most stable clusters; the thermodynamics and the rate constants of the most likely reactions; calculation of the impact velocities and hydrate distribution (PDF)

AUTHOR INFORMATION

Corresponding Author

*V. Loukonen. E-mail: ville.loukonen@aalto.fi.

Present Addresses

[‡]Infuser, Ole Maaløes Vej 5, bygning 779-3, 2200 Copenhagen, Denmark.

[§]Department of Applied Physics, COMP Centre of Excellence, Aalto University, P.O. Box 11100, FI-00076 Aalto, Espoo, Finland.

Notes

The authors declare no competing financial interest.

ACKNOWLEDGMENTS

The authors thank the ERC project 257360-MOCAPAF and the Academy of Finland through the centres of Excellence program (project No. 251748) for funding and the CSC-IT Centre for Science in Espoo, Finland, for computing time.

REFERENCES

(1) Seinfeld, J. H.; Pandis, S. N. *Atmospheric Chemistry and Physics: From air Pollution to Climate Change*, 2nd ed.; Wiley: Hoboken, NJ, 2006.

(2) Möhler, O.; Reiner, T.; Arnold, F. The Formation of SO_5^- by Gas Phase Ion–Molecule Reactions. *J. Chem. Phys.* **1992**, *97*, 8233–8239.

(3) Fehsenfeld, F.; Ferguson, E. Laboratory Studies of Negative Ion Reactions with Atmospheric Trace Constituents. *J. Chem. Phys.* **1974**, *61*, 3181–3193.

(4) Bork, N.; Kurtén, T.; Enghoff, M.; Pedersen, J.; Mikkelsen, K.; Svensmark, H. Structures and Reaction Rates of the Gaseous Oxidation of SO_2 by an $O_3^-(H_2O)_{0-5}$ Cluster - a Density Functional Theory Investigation. *Atmos. Chem. Phys.* **2012**, *12*, 3639–3652.

(5) Bork, N.; Kurtén, T.; Vehkamäki, H. Exploring the Atmospheric Chemistry of $O_2SO_3^-$ and Assessing the Maximum Turnover Number of Ion Catalyzed H_2SO_4 Formation. *Atmos. Chem. Phys.* **2013**, *13*, 3695–3703.

(6) Bork, N.; Loukonen, V.; Vehkamäki, H. Reactions and Reaction Rate of Atmospheric SO_2 and $O_3^-(H_2O)_n$ Collisions via Molecular Dynamics Simulations. *J. Phys. Chem. A* **2013**, *117*, 3143–3148.

(7) Tsona, T. N.; Bork, N.; Vehkamäki, H. On the Gas-Phase Reaction between SO_2 and $O_2^-(H_2O)_{0-3}$ Clusters - an ab initio Study. *Phys. Chem. Chem. Phys.* **2014**, *16*, 5987–5992.

(8) Tsona, T. N.; Bork, N.; Vehkamäki, H. Exploring the Chemical Fate of the Sulfate Radical Anion by Reaction with Sulfur Dioxide in the Gas Phase. *Atmos. Chem. Phys.* **2015**, *15*, 495–503.

(9) VandeVondele, J.; Krack, M.; Mohamed, F.; Parrinello, M.; Chassaing, T.; Hutter, J. QUICKSTEP: Fast and Accurate Density Functional Calculations using a Mixed Gaussian and Plane Waves Approach. *Comput. Phys. Commun.* **2005**, *167*, 103–128.

(10) Lippert, G.; Hutter, J.; Parrinello, M. A Hybrid Gaussian and Plane Wave Density Functional Scheme. *Mol. Phys.* **1997**, *92*, 477–488.

(11) VandeVondele, J.; Hutter, J. Gaussian Basis Sets for Accurate Calculations on Molecular Systems in Gas and Condensed Phases. *J. Chem. Phys.* **2007**, *127*, 114105.

(12) Goedecker, S.; Teter, M.; Hutter, J. Separable Dual-Space Gaussian Pseudopotentials. *Phys. Rev. B: Condens. Matter Mater. Phys.* **1996**, *54*, 1703–1710.

(13) Perdew, J. P.; Burke, K.; Ernzerhof, M. Generalized Gradient Approximation Made Simple. *Phys. Rev. Lett.* **1996**, *77*, 3865–3868.

(14) Grimme, S.; Antony, J.; Ehrlich, S.; Krieg, H. A Consistent and Accurate ab initio Parametrization of Density Functional Dispersion

Correction (DFT-D) for the 94 Elements H-Pu. *J. Chem. Phys.* **2010**, *132*, 154104.

(15) Elm, J.; Bilde, M.; Mikkelsen, K. V. Assessment of Density Functional Theory in Predicting Structures and Free Energies of Reaction of Atmospherical Prenucleation Clusters. *J. Chem. Theory Comput.* **2012**, *8*, 2071−2077.

(16) Leverentz, H. R.; Siepmann, J. I.; Truhlar, D. G.; Loukonen, V.; Vehkamäki, H. Energetics of Atmospherically Implicated Clusters Made of Sulfuric Acid, Ammonia, and Dimethyl Amine. *J. Phys. Chem. A* **2013**, *117*, 3819−3825.

(17) Bork, N.; Du, L.; Reiman, H.; Kurtén, T.; Kjaergaard, H. G. Benchmarking Ab Initio Binding Energies of Hydrogen-Bonded Molecular Clusters Based on FTIR Spectroscopy. *J. Phys. Chem. A* **2014**, *118*, 5316−5322.

(18) Falsig, H.; Gross, A.; Kongsted, J.; Osted, A.; Sloth, M.; Mikkelsen, K. V. Uptake of Phenol on Aerosol Particles. *J. Phys. Chem. A* **2006**, *110*, 660−670.

(19) Ma, X.; Chakraborty, P.; Henz, B. J.; Zachariah, M. R. Molecular Dynamic Simulation of Dicarboxylic Acid Coated Aqueous Aerosol: Structure and Processing of Water Vapor. *Phys. Chem. Chem. Phys.* **2011**, *13*, 9374−9384.

(20) Larson, L. J.; Kuno, M.; Tao, F.-M. Hydrolysis of Sulfur Trioxide to Form Sulfuric Acid in Small Water Clusters. *J. Chem. Phys.* **2000**, *112*, 8830−8838.

(21) Le Picard, S. D.; Tizniti, M.; Canosa, A.; Sims, I. R.; Smith, I. W. M. The Thermodynamics of the Elusive HO_3 Radical. *Science* **2010**, *328*, 1258−1262.

(22) Hoy, E. P.; Schwerdtfeger, C. A.; Mazziotti, D. A. Relative Energies and Geometries of the Cis- and Trans-HO_3 Radicals from the Parametric 2-Electron Density Matrix Method. *J. Phys. Chem. A* **2013**, *117*, 1817−1825.

(23) Varandas, A. J. C. On the Stability of the Elusive HO_3 Radical. *Phys. Chem. Chem. Phys.* **2011**, *13*, 15619−15623.

(24) Su, T.; Chesnavich, W. J. Parametrization of the Ion-Polar Molecule Collision Rate Constant by Trajectory Calculations. *J. Chem. Phys.* **1982**, *76*, 5183−5185.